SOVIET PHYSICS JETP VOLUME 11, NUMBER 4 OCTOBER, 1960

ELASTIC SCATTERING OF 240 – 330 Mev π^- MESONS BY HYDROGEN

V. G. ZINOV and S. M. KORENCHENKO

Joint Institute for Nuclear Research

Submitted to JETP editor November 13, 1959

J. Exptl. Theoret. Phys. (U.S.S.R.) 38, 1099-1105 (April, 1960)

Results of measurements of differential cross sections for the elastic scattering of π^- mesons of energies 240, 270, 307 and 333 Mev by hydrogen are given.

STUDY of the scattering of π^+ mesons by hydrogen in the energy region up to 360 Mev[1-3] has made it possible to establish the main features of the interaction of π mesons with nucleons in the states with isotopic spin $T = 3/2$. Until recently, very little was known about the interaction of π mesons with nucleons in the $T = 1/2$ states. The state with $T = 1/2$ enters only into scattering of negative π mesons. Determination of the contribution of these states in the energy region near resonance is practically impossible because of the overwhelming contribution of the interaction in $T = 3/2$, $j = 3/2$ states. It might be hoped that more specific information about the interaction in $T = 1/2$ states could be obtained at high energies. In connection with this, the authors carried out a systematic study of the interaction of π^- mesons with hydrogen in the energy range 240 – 330 Mev on the synchrocyclotron of the Joint Institute, using scintillation counters.

Preliminary results of this work have been given earlier.[4-7]

1. EXPERIMENTAL ARRANGEMENT

A detailed description of the apparatus and liquid-hydrogen target used has already been given by the authors.[8] Therefore, we limit ourselves to only a few remarks here.

The geometry of the experiment is shown in the figure. The beam of π^- mesons falling on the hydrogen target is detected by counters 1 and 2, connected in coincidence. The π mesons scattered at various angles are counted by two "angular" telescopes consisting of counters 3, 4 and 5, 6 connected in coincidence with counters 1, 2. In order to cut down the number of spurious coincidences, the counters 1 – 6 were connected in anticoincidence with counter 7, placed behind the target. This made it possible to decrease the background of random coincidences by a factor of 15 or 20, so that the number of random coincidences

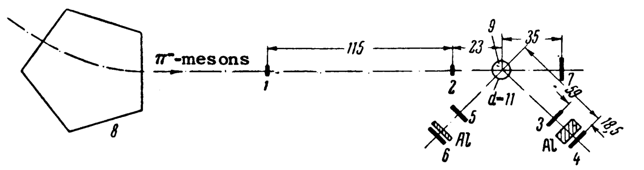

Geometry of the elastic-scattering experiment: 1, 2 – scintillation counters (6 × 6 cm); 3, 4, 5, 6 – scintillation counters (12.6 × 11.5 cm); 7 – anticoincidence counter (12.6 × 11.5 cm); 8 – deflecting magnet; 9 – liquid hydrogen.

did not exceed 4 to 7% of the scatterings from hydrogen. A special control was established so that the working intensity of the synchrocyclotron did not fluctuate more than 10% relative to the mean level. Therefore, the error in measurements arising from fluctuation in the background of random coincidences did not exceed ± 0.7%.

In the following, where four-fold coincidences 1234 or 1256 are referred to, coincidences of the type $1234\overline{7}$ and $1256\overline{7}$ are implied.

In measurement of the differential cross sections at 30, 45 and 60°, aluminum filters were placed in front of counters 4 and 6 to absorb recoil protons; the thicknesses of these filters at the various energies are given in Table I. In measurements at other angles, filters of thickness 5.4 g/cm² were always placed in front of counters 4 and 6 in order to decrease the background from low-energy particles.

2. MEASUREMENT OF THE DIFFERENTIAL CROSS SECTIONS FOR ELASTIC SCATTERING OF π^- MESONS OF ENERGIES 240, 270, 307 AND 333 Mev BY HYDROGEN

The angular distributions of π^- mesons scattered elastically by hydrogen were determined by measuring the ratios of four-fold coincidences Q in counters 1, 2, 3, 4 and 1, 2, 5, 6 to the two-fold coincidences D in counters 1 and 2. The measurements were carried out at 30, 45, 60, 80, 100, 125 and 150° in the l.s.

TABLE I. Thicknesses of aluminum filters for absorption of recoil protons (g/cm^2)

Angle in l.s., deg	240 Mev	270 Mev	307 Mev	333 Mev
30	16.2	21.6	28.4	31.0
45	10.8	14.8	20.2	21.6
60	5.4	8.1	9.4	10.8

All of the measurements were carried out in several series. Some of them were made simultaneously with the study of charge-exchange scattering of the π^- mesons. The measurements of a given series of the ratios Q/D for 240-Mev π^- mesons are given in Table II. The variation in observed values with change in energy is illustrated by the analogous Table III for 333 Mev. From Tables II and III it can be seen that at some angles the effect from hydrogen is two or more times smaller than the background from scattering of mesons off the walls of the target and counters.

TABLE II. Values of the ratio Q/D, observed at 240 Mev in one of the series of measurements

Angle in l.s., deg	$(Q/D) \times 10^6$ with H	$(Q/D) \times 10^6$ without H	Difference
30	144.3 ± 4.28	133.2±3.6	31.1±5.6
45	63.1 ± 2.0	36.5±1.5	26.6±2.5
60	47.5 ± 1.8	23.0±1.4	24.5±2.3
80	24.7 ± 1.6	10.8±1.1	13.9±2.0
100	23.1 ± 1.0	10.0±0.7	13.1±1.3
125	29.8 ± 1.6	13.0±0.7	16.6±2.0
150	48.0 ± 1.7	30.6±1.5	17.4±2.3

TABLE III. Values of the ratio Q/D, observed at 333 Mev in one of the series of measurements

Angle in l.s., deg	$(Q/D) \times 10^6$ with H	$(Q/D) \times 10^6$ without H	Difference
30	102.3 ± 3.3	73.5±3.2	28.7±4.6
45	53.1 ± 1.7	29.3±1.3	23.8±2.1
60	45.6 ± 2.1	27.3±1.7	18.3±2.7
80	29.6 ± 0.9	15.4±0.9	14.2±1.3
100	19.2 ± 1.2	10.4±1.1	8.8±1.6
125	21.0 ± 1.2	8.0±0.8	13.0±1.5
150	35.0 ± 2.2	26.0±2.1	9.0±3.0

Before beginning each series, the energy of π^- mesons in the beam was determined and the working of the apparatus was checked.

The differential cross sections were determined from the formula

$$\left(\frac{d\sigma}{d\Omega}\right)_{\text{lab}} = \frac{(Q/D)_{\text{diff}} - n_{\pi^0}}{N\Omega f h} \cdot 10^{-6}, \quad (1)$$

where $(Q/D)_{\text{diff}} = (Q/D)_{\text{with H}} - (Q/D)_{\text{without H}}$

is the effect per 10^6 counts of the monitor (mean weighted value for all of the series of measurements) with corrections to the observed values of Q/D for erroneous counts in the coincidences 1, 2; n_{π^0} is the effect produced by electrons and positrons from the decay of π^0 mesons (per 10^6 counts of the monitor); N is the mean number of hydrogen atoms per cm^2, this number being 0.447×10^{24} to an accuracy of ±1% for all energies; Ω is the solid angle subtended by the angular telescope; f is a correction to the observed cross section which is independent of scattering angle and h is a correction depending on angle of scattering.

The values of all terms in Eq. (1) are given in Tables IV — VII.

The n_{π^0} effect is composed of two parts. The main part is from electrons and positrons produced by conversion of γ rays from π^0 decays in hydrogen, walls of the target and counters 3 and 5. From measurements of exchange scattering, the effect of γ-ray conversion in a lead convertor of thickness 7.4 g/cm^2 is known at each angle. Knowing the cross sections for conversion and Compton effect in lead, carbon and hydrogen,[9,10] we can determine the number of electrons falling on the angular telescope to a sufficient accuracy. The counts produced by these electrons constituted 3.3 ± 1% of the counts observed in the same conditions with a lead convertor. In addition to electrons coming from conversion of γ rays, electrons produced[11] in ~ 1.6% of π^0 decays, $\pi^0 \to e^+ + e^- + \gamma$, were taken into account. In determining the n_{π^0} corrections, the absorption of electrons in the aluminum filters[10,12] placed between counters 3 and 4, and between 5 and 6, was taken into consideration.

The correction f, which did not depend on scattering angle, included corrections for the admixture of μ mesons in the beam and absorption of π^- mesons in counter 2, the front wall of the target, and in the hydrogen. The correction h, which depended upon angle, came mainly from the absorption of π mesons in the aluminum filter placed between the counters of the angular telescope. The magnitude of the absorption was determined experimentally by measuring Q/D with and without the aluminum filter. The measurements were carried out in the direct π^- beam with decreased intensity. The energies of the π^- mesons were chosen to correspond to those of π mesons scattered at the corresponding angle.

In addition to this main effect, the correction h also takes into account:

(a) absorption of the scattered π^- mesons in

TABLE IV. Differential cross sections for the elastic scattering of 240-Mev π^- mesons by hydrogen

Angle in l.s., deg	Ω, sr	$(Q/D)_{diff}$	n_{π^0}	f	h	$10^{27}(d\sigma/d\Omega)_{l.s.}$, cm²/sr	Angle in l.s., deg	$10^{27}(d\sigma/d\omega)$ in c.m.s., cm²/sr
30	0.0287	26.6±2.1	3.4	0.920	0.804	2.44±0.24	39.9	1.48±0.15
45	0.0342	25.8±1.7	3.0	0.920	0.848	1.91±0.17	58.7	1.30±0.12
60	0.0414	20.6±1.4	2.8	0.920	0.893	1.21±0.11	76.3	0.953±0.087
80	0.0414	13.4±1.3	1.5	0.920	0.900	0.779±0.090	97.8	0.763±0.088
100	0.0411	11.8±0.8	1.0	0.920	0.902	0.707±0.062	117.1	0.856±0.076
125	0.0410	15.3±0.9	0.9	0.920	0.904	0.945±0.078	138.6	1.44±0.12
150	0.0414	17.4±1.4	1.0	0.920	0.895	1.075±0.106	158.1	1.92±0.19

TABLE V. Differential cross sections for the elastic scattering of 270-Mev π^- mesons by hydrogen

Angle in l.s., deg	Ω, sr	$(Q/D)_{diff}$	n_{π^0}	f	h	$10^{27}(d\sigma/d\Omega)_{l.s.}$ cm²/sr	Angle in l.s., deg	$10^{27}(d\sigma/d\omega)$ in c.m.s. cm²/sr
30	0.0287	22.6±1.7	2.9	0.925	0.756	2.20±0.22	40.6	1.30±0.13
45	0.0342	21.2±1.6	2.8	0.925	0.811	1.60±0.15	59.6	1.07±0.10
60	0.0414	16.9±1.2	1.8	0.925	0.892	0.990±0.093	77.3	0.775±0.073
80	0.0414	9.8±1.1	1.0	0.925	0.899	0.574±0.071	98.8	0.563±0.073
100	0.0411	10.0±0.8	0.7	0.925	0.900	0.608±0.061	117.9	0.748±0.074
125	0.0410	11.1±0.8	0.7	0.925	0.905	0.678±0.057	139.3	1.06±0.09
150	0.0414	13.5±1.2	0.7	0.925	0.909	0.819±0.086	158.4	1.51±0.16

TABLE VI. Differential cross sections for the elastic scattering of 307-Mev π^- mesons by hydrogen

Angle in l.s., deg	Ω, sr	$(Q/D)_{diff}$	n_{π^0}	f	h	$10^{27}(d\sigma/d\Omega)_{l.s.}$, without correction for meson production cm²/sr	Correction to $10^{27}(d\sigma/d\Omega)_{l.s.}$ for meson production, cm²/sr	Angle in c.m.s. deg	$10^{27}(d\sigma/d\omega)$ in c.m.s. cm²/sr
30	0.0340	27.5±2.6	3.4	0.934	0.724	2.34±0.27	0.052±0.040	41.3	1.31±0.16
45	0.0413	24.3±2.3	2.0	0.934	0.774	1.67±0.19	0.053±0.040	60.6	1.06±0.13
60	0.0413	16.8±1.2	1.3	0.934	0.865	1.04±0.106	0.066±0.050	78.5	0.752±0.091
80	0.0513	11.5±0.9	0.8	0.934	0.909	0.548±0.048	0.043±0.028	100.0	0.500±0.056
100	0.0513	10.4±0.9	0.5	0.934	0.895	0.515±0.054	0.017±0.017	119.0	0.625±0.072
125	0.0513	11.4±1.1	0.4	0.934	0.893	0.574±0.065	0.002±0.002	140.0	0.923±0.105
152	0.0494	11.4±1.0	0.5	0.934	0.893	0.594±0.062	0	160.3	1.15±0.12

TABLE VII. Differential cross sections for the elastic scattering of 333-Mev π^- mesons by hydrogen

Angle in l.s., deg	Ω, sr	$(Q/D)_{diff}$	n_{π^0}	f	h	$10^{27}(d\sigma/d\Omega)_{l.s.}$ without correction for meson production cm²/sr	Correction to $10^{-27}(d\sigma/d\Omega)_{l.s.}$ for meson production, cm²/sr	Angle in c.m.s. deg	$10^{27}(d\sigma/d\omega)$ in c.m.s. cm²/sr
30	0.0340	27.1±1.5	3.2	0.939	0.728	2.30±0.24	0.12±0.06	41.9	1.22±0.14
45	0.0413	22.8±1.3	2.3	0.939	0.799	1.48±0.12	0.13±0.06	61.3	0.874±0.093
60	0.0413	16.2±1.3	1.4	0.939	0.871	0.985±0.084	0.11±0.05	79.2	0.675±0.076
80	0.0511	12.8±0.8	0.9	0.939	0.919	0.604±0.046	0.093±0.03	100.8	0.508±0.055
100	0.0511	9.47±0.75	0.4	0.939	0.900	0.470±0.038	0.056±0.028	119.7	0.527±0.060
125	0.0511	11.7±0.9	0.4	0.939	0.883	0.595±0.057	0.017±0.007	140.6	0.954±0.096
150	0.0511	9.32±1.13	0.3	0.939	0.896	0.468±0.052	0.004±0.002	159.2	0.914±0.104

hydrogen (mainly because of charge-exchange scattering), scattering of π^- mesons in the walls of the target and counters 3 and 5; the size of this correction was 2 — 4%.

(b) random coincidences in counters 1, 2, 3, 4 and 1, 2, 5, 6 of the type of coincidences 123 of the recoil proton accompanied by a spurious particle traversing counter 4 (this correction did not exceed 1% of that from the hydrogen).

(c) a geometrical factor — a small (not larger than 1.2%) change in the observed cross section as compared with the true one, coming from the finite dimensions of the counters, which means that the measured cross section was averaged over an angle of 13 – 15°.

At 307 and 333 Mev it was already necessary to take into account processes in which charged mesons are produced by the π^- mesons. The contribution from these processes at 80° in the l.s. was determined experimentally.[8] For the other angles, corrections for this effect were made under the following schematic assumptions: the angular distribution of mesons participating in inelastic processes is isotropic in the c.m.s.; the energy spectrum of these mesons has the form of an isosceles triangle. The corrections to the differential cross section in the l.s., calculated under these assumptions, are given in Tables VI and VII.

The errors in the differential cross sections, shown in Tables IV – VII, include, in addition to statistical errors, errors in the determination of terms which enter into Eq. (1). The contributions from individual effects to these errors for 270 Mev are given in Table VIII. At different energies, the errors differ only little from those given in this table.

The c.m.s. angles and differential cross sections are given in the two last columns of Tables IV – VII.

Additional measurements of the cross section for π^- elastic scattering were carried out at 80° in the l.s. at 270, 307 and 333 Mev using the method of conjugate telescopes, i.e., the scattered π^- meson was detected in coincidence with the recoil proton. Because of this, the background was a factor of about five less than the scattering from hydrogen. In processing these results, practically the same corrections as in the processing of data obtained by the usual means were made. The only difference was that, instead of corrections for the conversion of γ rays, a correction was introduced into h for absorption of recoil protons (1.4 – 1.9%) in the hydrogen and in the walls of the target. The production of mesons by mesons obviously does not have to be taken into account.

The results of these measurements and the corrections carried out are given in Table IX. The differential cross section in the c.m.s., obtained by averaging the results of measurements carried out in the usual way and by the method of conjugate telescopes, is given in the last column.

3. CONCLUSIONS

We represent now the angular distribution of elastically scattered mesons in the c.m.s. as a sum of three Legendre polynomials:

$$\frac{d\sigma}{d\omega} = A_0^- + A_1^- P_1(\cos\vartheta) + A_2^- P_2(\cos\vartheta). \tag{2}$$

The values of the coefficients A_i^- (in cm^2 sr^{-1})

TABLE VIII. Individual effects (in percentages of the differential cross section) entering into the errors in the differential cross sections at 270 Mev

Angle in l.s., deg	Δn_{π^0}	Correction for the Al filter	Geometrical factor	Effect of anticoincidence	Random coincidence	Absorption of the beam in the walls of the target and counter 2	False counts in the coincidences 1, 2	Inhomogeneity of the beam and inaccuracies in the determination of the solid angles	Absorption in counters 4 and 6 and in the walls of the target	Total error
30	4.2	3	1	1	1	0.5	1	3	0.5	6.3
45	4.4	2.5	1	1	1	0.5	1.5	3	0.8	6.4
60	3.5	2.5	1	1	1	0.5	1.5	3	0.8	5.8
80	3.3	2	1	1	1	0.5	1.5	3	0.8	5.6
100	2.3	2	1	1	1	0.5	1.5	3	0.8	5.0
125	2.1	2	1	1	1	0.5	1.5	3	0.5	4.9
150	1.8	2	1	1	1	0.5	1	3	0.5	4.8

TABLE IX. Differential cross sections for elastic π^--meson scattering by hydrogen at 80° l.s. and 270, 307 and 333 Mev, obtained by the method of conjugate telescopes

Energy of π^- mesons, Mev	Ω, sr	$(Q/D)_{\text{diff}}$	f	h	$10^{27}(d\sigma/d\Omega)_{\text{l.s.}}$, cm^2/sr	Angle in c.m.s., degrees	$10^{27}(d\sigma/d\omega)_{\text{c.m.s.}}$, obtained by the method of conjugate telescopes, cm^2/sr	$10^{27}(d\sigma/d\omega)_{\text{c.m.s.}}$, mean value, cm^2/sr
270	0.0344	7.66±0.72	0.925	0.879	0.613±0.065	98.8	0.601±0.065	0.585±0.053
307	0.0417	7.91±0.30	0.934	0.894	0.508±0.038	100.0	0.502±0.038	0.501±0.032
333	0.0417	8.03±0.31	0.939	0.907	0.506±0.037	100.8	0.503±0.037	0.505±0.032

TABLE X. Coefficients of the angular distribution of π^- mesons (10^{-27} sr^{-1})

Energy of π^- mesons, Mev	A_0^-	A_1^-	A_2^-	M	M_0, expected	$\sigma_{\pi^-\to\pi^+} = 4\pi A_0^-$, 10^{-27} cm^2
240	1.20 ± 0.06	0.17 ± 0.11	0.89 ± 0.15	5.67	4	15.1 ± 0.8
270	0.99 ± 0.05	0.21 ± 0.09	0.74 ± 0.12	2.80	4	12.4 ± 0.6
307	0.91 ± 0.06	0.38 ± 0.11	0.72 ± 0.11	2.09	4	11.4 ± 0.8
333	0.82 ± 0.05	0.32 ± 0.06	0.57 ± 0.10	4.54	4	10.3 ± 0.6

calculated by the least squares method, are given in Table X. These coefficients give the minimum value of the sum of weighted squares of deviations

$$M = \sum \left(\frac{\sigma_i - f_i}{\varepsilon_i}\right)^2, \tag{3}$$

where f_i is the differential cross section at the i-th angle calculated from Eq. (2), σ_i is the experimental value of the differential cross section, and ϵ_i is the error in the measured differential cross section.

According to the theory of errors,[13,14] with the correct relation between experimental points, the most probable value of M is roughly equal to the difference between the number of experimental points and the number of parameters fitted. In our case, this number is four at all energies. Comparison of the expected values of M and those obtained (Table X) shows that the experimental values of the differential cross sections satisfy the dependence Eq. (2) sufficiently well.

Integrating the angular distribution of Eq. (2), one obtains the total cross section for elastic scattering of π^- mesons by protons. Integration leads to the expression

$$\sigma_{\pi^-\to\pi^-} = 4\pi A_0^-.$$

The magnitudes of the total cross sections obtained in this way are given in the last column of Table X.

[1] Mukhin, Ozerov, and Pontecorvo, JETP **31**, 371 (1956), Soviet Phys. JETP **4**, 237 (1957).

[2] A. I. Mukhin and B. Pontecorvo, JETP **31**, 550 (1956), Soviet Phys. JETP **4**, 373 (1957).

[3] E. L. Grigor'ev and N. A. Mitin, JETP **32**, 445 (1957), Soviet Phys. JETP **5**, 378 (1957).

[4] V. G. Zinov and S. M. Korenchenko, JETP **33**, 335 (1957), Soviet Phys. JETP **6**, 260 (1958).

[5] V. G. Zinov and S. M. Korenchenko, JETP **33**, 1308 (1957), Soviet Phys. JETP **6**, 1007 (1958).

[6] V. G. Zinov and S. M. Korenchenko, JETP **33**, 1307 (1957), Soviet Phys. JETP **6**, 1006 (1958).

[7] V. G. Zinov and S. M. Korenchenko, JETP **36**, 618 (1959), Soviet Phys. JETP **9**, 429 (1959).

[8] V. G. Zinov and S. M. Korenchenko, JETP **34**, 301 (1958), Soviet Phys. JETP **7**, 210 (1958).

[9] I. L. Lawson, Phys. Rev. **75**, 433 (1949).

[10] De Wire, Ashkin, and Beacher, Phys. Rev. **83**, 505 (1951).

[11] Lindenfeld, Sachs, and Steinberger, Phys. Rev. **89**, 531 (1953).

[12] Davies, Bethe, and Maximon, Phys. Rev. **93**, 788 (1954).

[13] I. V. Dunin-Barkovskiĭ and N. V. Smirnov, Теория вероятностей и математичемкая статистика в технике (Theory of Probability and Mathematical Statistics in Technology) Gostekhizdat, 1955.

[14] M. E. Rose, Phys. Rev. **91**, 610 (1953).

Translated by G. E. Brown
218

ERRATA TO VOLUME 10

page	reads	should read
Article by A. S. Khaĭkin		
1044, title	. . . resonance in lead	. . . resonance in tin
6th line of article	~ 1000 oe	~ 1 oe
Article by V. L. Lyuboshitz		
1223, Eq. (13), second line	$\ldots-\mathrm{Sp}_{1,2}\mathscr{E}(\mathbf{e}_1)$	$\ldots-\mathrm{Sp}_{1,2}\mathscr{E}(\mathbf{e}_2)\ldots$
1226, Eq. (26), 12th line	$\cdots\{(\mathbf{p}+\mathbf{q},\ \mathbf{p}$	$\cdots\{(\mathbf{p}+\mathbf{q},\mathbf{p})-(\mathbf{p}+\mathbf{q},\ \mathbf{n})\cdot$ $\cdot(\mathbf{pn})\}$
1227, Eqs. (38), (41), (41a) numerators and denominators	$(\mathbf{p}^2-\mathbf{q})$	$(\mathbf{p}^2-\mathbf{q}^2)^2$
1228, top line	$\mathbf{m}_2=\frac{\mathbf{q}_1-\mathbf{p}_1}{\mathbf{q}_1-\mathbf{p}_1}$	$\mathbf{m}_2=[\mathbf{m}_3\ \mathbf{m}_1]$

ERRATA TO VOLUME 12

page	reads	should read
Article by Dzhelepov et al.		
205, figure caption	54	5.4
Article by M. Gavrila		
225, Eq. (2), last line	$-2\gamma\Theta^{-4}\,{}^1\!/_8$	$-2\gamma\Theta^{-4}-{}^1\!/_8$
Article by Dolgov-Savel'ev et al.		
291, caption of Fig. 5, 4th line	$p_0 = 50 \times 10^{-4}$ mm Hg	$p_0 = 5 \times 10^{-4}$ mm Hg.
Article by Belov et al.		
396, Eq. (24) second line	$\ldots-(4-2\eta)\,\sigma_1+\ldots$	$\ldots+(4-2\eta)\,\sigma_1+\ldots$
396, 17th line (r) from top	. . less than 0.7	. . less than 0.07
Article by Kovrizhnykh and Rukhadze		
615, 1st line after Eq. (1)	$\omega_{0e}^2=2\pi e^2 n_e/m_e,$	$\omega_{0e}^2=4\pi e^2 n_e/m_e,$
Article by Belyaev et al.		
686, Eq. (1), 4th line	$\ldots b_{\rho_2 m_2}(s_2')+\cdots$	$\ldots b_{\rho_1 m_1}(s_1')+\cdots$
Article by Zinov and Korenchenko		
798, Table X, heading of last column	$\sigma_{\pi^-\to\pi^+}=$	$\sigma_{\pi^-\to\pi^-}=$
Article by V. M. Shekhter		
967, 3d line after Eq. (3)	$\varepsilon\equiv 2m_pE+m_p^2$	$\varepsilon\equiv(2m_pE+m_p^2)^{1/2}$
967, Eq. (5), line 2	$+(B_V^2+B_A^2)\ldots$	$+(B_V^2+B_A^2)\,Q\ldots$
968, Eq. (7)	$\ldots(C_V^2+C_A^2).$	$\ldots C_V^2+C_A^2-Q^2(B_V^2+B_A^2).$
968, line after Eq. (7)	for $C_V^2+C_A^2\equiv\ldots$	for $C_V^2+C_A^2$ $-Q^2(B_V^2+B_A^2)\equiv\ldots$
Article by Dovzhenko et al.		
983, 11th line (r)	$\gamma=1.8\pm$	$\gamma=1{,}8\pm0{,}2$
Article by Zinov et al.		
1021, Table XI, col. 4	—1,22	1,22
Article by V. I. Ritus		
1079, line 27 (l)	$-\Lambda_{\pm}(t),$	$\Lambda_{\pm}(t),$
1079, first line after Eq. (33)	$\frac{1}{2}(1+\beta).$	$\frac{1}{2}(1\pm\beta).$
1079, 3d line (l) from bottom	$\ldots\mathfrak{N}(q'p;\ pq')\ldots$	$\ldots\mathfrak{N}(p'q;\ pq')\ldots$
Article by R. V. Polovin		
1119, Eq. (8.2), fourth line	$U_{0x}u_xg(\gamma)-[\gamma\cdots$	$-U_{0x}u_xg(\gamma)\,[\gamma\cdots$
1119, Eq. (8.3)	$\cdots$sign $u.$	$\cdots$sign $u_g.$
Article by V. P. Silin		
1138, Eq. (18)	$\cdots+\frac{4}{5}c^2k^2$	$\cdots+\frac{6}{5}c^2k^2.$